0090-9556/00/2810-1255–1261$03.00/0
DRUG METABOLISM AND DISPOSITION
Vol. 28, No. 10
1803/850741
Printed in U.S.A.

DMD 28:1255–1261, 2000

DISPOSITION AND TOXICITY OF A MIXED BACKBONE ANTISENSE OLIGONUCLEOTIDE, TARGETED AGAINST HUMAN CYTOMEGALOVIRUS, AFTER INTRAVITREAL INJECTION OF ESCALATING SINGLE DOSES IN THE RABBIT

BARRY H. DVORCHIK AND JUDITH K. MARQUIS

Hybridon, Inc., Milford, Massachusetts

(Received October 1, 1999; accepted June 22, 2000)

This paper is available online at http://www.dmd.org

ABSTRACT:

The ocular disposition and toxicity of GEM132, a mixed backbone phosphorothioate oligonucleotide developed for the treatment of cytomegalovirus-induced retinitis, were studied in rabbits for 6 months following single intravitreal injection of 5, 20, or 100 μg/eye (toxicity) and 3.7, 15.7, or 78.5 μg/eye (disposition). Intraocular pressure, electroretinograms, and ophthalmoscopy were evaluated in the toxicity arm as well as gross and microscopic pathology at the termination of the study. Vitreous humor, retina, and the remaining ocular tissues were collected from all animals in the disposition arm. No toxicities were observed in the low-dose group. Intraocular pressure was transiently mildly increased in the mid- and high-dose groups; macroscopic findings were mild and infrequent. Changes in electroretinograms and histopathological findings attributed to GEM132 were observed by 4 weeks postdose in the high-dose group. Area under the curve values in all ocular tissues sampled were proportional to dose, suggesting GEM132 disposition exhibited first-order kinetics. Vitreous humor concentrations decreased in a multiphasic manner, consistent with rapid distribution. Polyacrylamide gel electrophoresis analysis of retinal extracts indicated that, at 4 weeks postdose, 90% of the radioactivity was associated with parent compound. At 8 weeks postdose, this had decreased to 70%, and subsequently to 50% at 21 weeks postdose. In retina, GEM132 reached concentrations >5 times IC_{90} by 1 week postdose, with maximum concentrations 4 to 8 weeks postdose. Retinal concentrations of intact GEM132 then declined at a very slow rate. Microautoradiography suggested that radioactivity was distributed throughout the retinal layers, the largest amount being located in the middle layers.

The advancement of antisense oligonucleotides to human clinical trials as anticancer (Bayever et al., 1993; Stevenson et al., 1999; Chen et al., 2000), anti-inflammatory (Glover et al., 1997), or antiviral (Perry and Balfour, 1999; Séréni et al., 1999) therapeutics has been greatly enhanced by progress in the synthesis of nuclease-resistant oligonucleotides and an understanding of their pharmacological properties. Most antisense oligonucleotides in clinical trials are phosphorothioate (PS)[1] oligonucleotides, DNA molecules in which single nonbridging oxygen has been replaced by sulfur. This modification results in enhanced resistance to endonucleases, the enzymes primarily responsible for the catabolism of oligonucleotides. Studies with mixed backbone oligonucleotides (MBOs) where there is a substitution of the 2′-position of ribose with alkyl substituents appear to hold promise of increased safety and more desirable pharmacokinetic properties, including a greater resistance to endonucleases than PS oligonucleotides (Agrawal et al., 1997a; Chen et al., 2000).

Human cytomegalovirus (HCMV), a common opportunistic infection in immunocompromised persons, is a major cause of life-threatening disease. CMV-induced retinitis, if left untreated, will cause severe, irreversible damage to the retina, resulting in progressive loss of vision in the involved eye(s). Currently available therapies for CMV-induced retinitis include ganciclovir, foscamet, cidofovir, and the recently approved PS antisense oligonucleotide, fomivirsen (ISIS 2922).

GEM132 is a 20-mer mixed backbone oligonucleotide (MBO) with 2′-*O*-methylribonucleosides at the two 3′- and four 5′-terminal nucleotides. It is antisense, complementary to the intron-exon boundary of the UL35 and UL37 premRNA transcripts of HCMV, and has shown antiviral activity in vitro with an IC_{90} of about 0.1 μM against standard laboratory strains of the virus (Pari et al., 1995). Viruses resistant to current therapies do not show cross-resistance to GEM132, which has shown activity against a battery of over 20 clinical HCMV isolates with an IC_{90} of about 0.1 μM (Field et al., 1997). GEM132 has entered clinical trials as an antiviral for patients with HCMV-induced retinitis who can no longer benefit from or tolerate available therapies.

Although studies have been published on the pharmacokinetics of PS oligonucleotides after intravitreal dosing (Leeds et al., 1997, 1998), none have described the disposition and toxicity of an MBO after intravitreal administration. Because GEM132 had prolonged persistence in tissues after i.v. administration to rats (Hybridon internal report), this investigation was designed to characterize the acute and chronic toxicity and disposition of GEM132 in Dutch Belted rabbits for 6 months after a single intravitreal dose.

Materials and Methods

Synthesis and Purification of GEM132. GEM132 is a 20-base phosphorothioate MBO (5′-UGGGGCTTACCTTGCGAACA-3′), 6605-Da molecular

[1] Abbreviations used are: PS, phosphorothioate; HCMV, human cytomegalovirus; ERG, electroretinogram; MBO, mixed backbone oligonucleotide; PAGE, polyacrylamide gel electrophoresis; AUC, area under the curve.

Send reprint requests to: Barry H. Dvorchik, Ph.D., Barry Dvorchik & Associates, Inc., 5809 Piney Lane Dr., Suite 105, Tampa, FL 33625. E-mail: bdvorchik@email.msn.com

mass (free acid), in which two deoxynucleosides at the 5′ end and four deoxynucleosides at the 3′ end (underlined) are substituted with 2′-*O*-methylribonucleosides. GEM132 was chemically synthesized using deoxynucleoside phosphoramidites (Milligen, Milford, MA) and 2′-*O*-methylribonucleoside phosphoramidites (Glen Research, Sterling, VA) on an automated synthesizer as previously described (Padmapriya et al., 1994; Zhang et al., 1995) and purified by preparative reversed phase HPLC. The purity was 91% as determined by capillary gel electrophoresis. Radiolabeled GEM132 (specific activity, 15 μCi/mg) was synthesized with [4,6-^{14}C]thymidine phosphoramidite. The radiolabel was located in the first thymidine from the 5′ end. Purity was 90% by capillary gel electrophoresis.

Experimental Design. Male Dutch Belted rabbits were given a single intravitreal injection (50 μl) of GEM132 in both eyes. Control animals received saline only. For the disposition study, [^{14}C]GEM132 was administered; eyes and selected tissues were harvested at various times postdosing ($n = 3$ eyes/time point). The oligonucleotide was dissolved in 0.9% saline, and the doses administered were 3.7 μg/eye (0.07 μCi), 15.7 μg/eye (0.3 μCi), and 78.5 μg/eye (1.5 μCi). For the toxicity study, unlabeled GEM132 was administered at doses of 5, 20, or 100 μg/eye.

Electroretinograms (ERGs). Electroretinograms were obtained from all animals in the study at regular intervals. Light stimuli included scotopic blue, red, and white single flash and 30 Hz white flicker. The animals were anesthetized with ketamine (50 mg/kg)/xylazine (5 mg/kg) and dark-adapted at least 30 min before recording of the ERG. A mydriatic agent was applied to the eyes to dilate the pupils before testing.

Sample Processing and Storage Conditions. At each time point, the left eye from the even-numbered animals and both eyes from the odd-numbered animals were dissected, and retina, vitreous humor, and remaining ocular tissue were removed and weighed. The weighed vitreous humor (0.724 ± 0.031 g, mean ± S.D.) and retina (0.0283 ± 0.0003 g) samples were homogenized in 2 ml of 0.9% saline in preweighed glass tubes with a Teflon probe. After homogenization, aliquots of retina were solubilized in 35% tetraethylammonium hydroxide. Ten milliliters of Hionic Fluor scintillation fluid (Canberra Packard, Ontario, Canada) was added to vitreous humor and solubilized retina, and radioactivity was measured by liquid scintillation spectroscopy. Remaining ocular tissue samples (1.47 ± 0.18 g) were minced and digested in toto in 35% tetraethylammonium hydroxide. Duplicate aliquots of the digest were added to 10 ml of scintillation fluid, and radioactivity was determined. Samples having a radioactivity level of less than or equal to double background were considered below the limit of quantitation and considered zero.

Autoradiography and Microautoradiography Conditions. At each time point, the right eye of each even-numbered animal was removed and fixed in a 2.5% gluteraldehyde solution, stored, refrigerated, and transferred within 24 h to 10% neutral buffered Formalin where they remained for at least 24 h before trimming. Eyes were then trimmed, dehydrated, infiltrated, and imbedded in paraffin within 8 days after necropsy. Six-micrometer-thick sections were prepared. The following procedures were conducted under reduced safety light conditions: sections were subjected to deparaffination, dipped in diluted and warmed Kodak NTB-2 nuclear track emulsion, followed by a 30-min rinse in hot distilled water and controlled drying. After drying, the emulsion-coated slides were stored in lightproof plastic boxes at 4–8°C. All slides were developed after 15 days of exposure using a solution of Kodak D-19 developer, washed, fixed in Kodak Rapid Fixer, and washed. Slides were stained with H&E, mounted, and evaluated for the localization and relative concentration of radioactivity (visualized as small, reduced silver grains lying on cellular surfaces). A four-grade (1, slight; 2, mild; 3, moderate; and 4, severe) grading scheme was used to semiquantify the amount of radioactivity. The amount of radioactivity present in underlying sclera was used to establish a threshold between a negative and a slight deposition of radioactivity in the retina.

Polyacrylamide Gel Electrophoresis (PAGE) and Phosphor Image Analysis. Retinal homogenates were subjected to protein digestion by incubation with proteinase K enzyme (0.25 ml of a 20 mg/ml solution) containing 20 mM Tris EDTA for 3 h at 60°C. Samples were extracted twice with Tris ETDA-saturated phenol-chloroform solution (1:1, v/v) and once with chloroform to remove proteinase K, digested protein, and lipids from nucleic acids. After extraction, an aliquot of the organic and aqueous phase from each sample was removed, and total radioactivity was determined by liquid scintillation spectroscopy. This allowed for the determination of extraction recovery. The average recoveries (±S.D.) were 79.7 ± 13.2% (quality control standards), 74.3 ± 19.1% (day 7), 75.7 ± 6.4% (day 14), 72.4 ± 10.3% (day 28), 74.1 ± 8.2% (day 56), 87.3 ± 3.6% (day 114), and 87.4 ± 12.0% (day 149). No radioactivity (≥2× background) was measurable in the organic phase, indicating that all the GEM132-associated radioactivities were retained in the aqueous phase following extraction. Loss of radioactivity was believed to be due to the difficulty in completely separating the two phases; a thin layer of the aqueous phase was always left behind. An 8-μl aliquot of the aqueous phase was loaded on a 20% polyacrylamide gel containing 7.5 μM urea and subjected to electrophoresis (70–290 V, 3–14 mA, 60–153 min). Quality control standards (0.11, 0.60, and 4.1 mg/ml, corresponding to 780, 4,500, and 21,000 dpm) were prepared by adding known amounts of radiolabeled GEM132 to retinal homogenates obtained from control rabbits. Duplicate standards were loaded on each of the two outer channels of the gel. After electrophoresis, Southern blots of the gels were performed on 0.45-μ nitrocellulose membranes over a period of about 12 h. The nitrocellulose membranes were then removed and allowed to dry at room temperature. Membranes were exposed to the phosphor screen for 25 to 288 h (Molecular Dynamics Storage Phosphor Screen, Sunnyvale, CA) at room temperature, after which the phosphor screen was scanned by a phosphor imager (Molecular Dynamics Phosphor Imager SI) to obtain radioactivity profiles. The lower limit of detection was determined to be an area of ≥15 phosphor image units. Concentrations of intact GEM132 were calculated by multiplying the measured total radioactivity in the retina (total MBO) by the fraction eluting with the same mobility as the standards, as determined by PAGE/phosphor image analysis and correcting for purity (90%).

Intergel variability and intragel variability were determined for phosphor image analysis. Intergel variability ranged from 8.6 to 5.3%. For intragel variability, the %CV for four samples processed on the same gel ranged from 5.5 to 11.1%. The limit of quantification for phosphor image analysis, determined for four different exposure times, was as follows: 295 dpm (24 h), 200 dpm (48 and 96 h), and 100 dpm (144 h).

Results

Ophthalmic Examinations. Signs of ocular irritation attributed to the injection of GEM132 were infrequent, mild, and transient. Mild cellular infiltrate in the anterior vitreous occurred almost exclusively in the high-dose animals from 2 to 16 weeks postdose. Signs of iritis were also mild and infrequent. Retinal lesions were observed almost exclusively in the high-dose animals. Changes in intraocular pressures were mild and transient and considered only potentially related to treatment.

Electroretinograms. Representative data for ERGs are shown in Table 1. The scotopic white flash measures the response of both rods and cones and is representative of overall retinal function. The mean values and standard deviations for B-wave amplitude and response latency both demonstrate significant dose-related decreases. No changes were observed in the low-dose animals for any ERG parameter, when compared with controls. Statistically significant changes that were observed in the mid-dose animals included a decrease in amplitude in the scotopic blue and red parameters during weeks 4 to 20, decreased latency in the scotopic red parameter during week 10, and decreased amplitude in the scotopic white parameter, weeks 10 to 20. Statistically significant changes occurred in both amplitude and latency for all parameters (scotopic blue, red, white and white flicker) at all time points measured in the high-dose animals. Due to the severely decreased ERG potential observed at 16 weeks in the high-dose group, we chose to terminate this group at this time. The decreased ERG potential that persisted for up to 20 weeks in the mid-dose group was the reason we chose to terminate the mid- and low-dose groups at week 21.

Histopathology. Histopathological findings attributed to the administration of GEM132 were seen in the retina, lens, and optic nerve of a few animals in the mid-dose group at 8 and 21 weeks and the high-dose group at 4, 8, and 16 weeks postdose. Slight retinal degen-

TABLE 1

Summary of electroretinograph data following a single intravitreal injection of GEM 132 (scotopic white, single flash)

Group	Dose		Week 4		Week 8		Week 12		Week 20	
			Amplitude	Latency	Amplitude	Latency	Amplitude	Latency	Amplitude	Latency
			μV	*ms*	μV	*ms*	μV	*ms*	μV	*ms*
1	Vehicle	Mean	145.94	26.61	162.17	26.67	172.09	31.17[a]	180.25	28.67
		S.D.	56.13	5.14	71.39	5.30	36.66	7.28	30.89	5.51
2	GEM132 (5 μg/eye/injection)	Mean	158.39	27.34	171.65	25.25	174.35	26.25	178.16	26.08
		S.D.	45.24	5.88	30.63	1.64	49.53	1.51	25.67	0.58
3	GEM132 (20 μg/eye/injection)	Mean	122.37	24.17	115.30	24.75	98.85[a,b]	25.75[a]	97.72[a,b]	25.08
		S.D.	41.75	3.59	70.12	1.14	49.52	2.04	52.97	1.72
4	GEM132 (100 μg/eye/injection)	Mean	46.35[b]	17.64[c]	20.30[a,b]	14.88[c]	25.75[b]	9.92[c]	Not measured	Not measured
		S.D.	52.78	10.82	29.36	9.07	35.22	12.38		

[a] Statistically significant from week 4, $P < .05$ (*t* test).
[b] Statistically significant from group 1, $P < .05$ (Dunnett's test).
[c] Statistically significant from group 1, $P < .05$ (Wilcoxon test).

eration characterized by partial disorganization of the inner and outer plexiform layer and the ganglion cell layer was observed in one high-dose animal at week 4 and in three high-dose animals at week 8. This finding was also observed in one mid-dose animal at weeks 8 and 21 and in one control and two low-dose animals at week 21. Retinal detachment was observed in one high-dose animal at week 8. A basophilic granular material was observed in the retina of one high-dose animal at week 4, in three high-dose animals at week 8, and in two high-dose animals at week 16. One mid-dose animal at week 8 also presented with this finding. A slight to mild mononuclear infiltration was seen in the optic nerves of some high-dose animals at weeks 4 and 6 and in one high-dose animal at week 16. This was also observed in some mid-dose animals at week 8.

Systemic Exposure following Intravitreal Administration. Plasma concentrations of total radioactivity were lower by 3 to 4 orders of magnitude compared with that in ocular tissues. GEM132-derived radioactivity in tissues such as kidneys, liver, and spleen was also low compared with that in ocular tissues. The highest concentration of radioactivity in nonocular tissues was seen in the liver 14 days postdose and equaled 2.3% of the intraocular dose.

Disposition Kinetics of GEM132-Derived Radioactivity in Vitreous Humor. AUC values in vitreous humor increased somewhat less than proportional to dose (Table 2). GEM132-derived radioactivity was cleared rapidly from the vitreous humor (Fig. 1). At 7 days postdose, ≥93% of the dose had cleared the vitreous humor, which increased to ≥99% of the dose by 28 days postdose. Radioactivity distributed rapidly throughout the tissues of the eye (Table 3).

Disposition Kinetics and Metabolism of GEM132-Derived Radioactivity in Retina. The AUC values in retina increased approximately in proportion to the dose (Table 2). The profiles of radioactivity by PAGE/phosphor image analysis of retina homogenates are presented in Table 4. Figure 2 shows representative electropherograms from different gels. Differences in the mobility of the calibration standard from gel to gel were corrected by running calibration standards with each gel. There was no apparent difference in the recoveries at each sampling time between dose groups or, overall, between samples of retina homogenates spiked with radiolabeled GEM132. At day 7 postdose, all extracted radioactivities migrated with the same mobility as GEM132. From day 14 to day 149 postdose, the mean radioactivity in extracted samples with a mobility similar to GEM132 declined to 45.1% on day 149. In the low- and mid-dose groups, radioactivity associated with shorter chain length oligonucleotides was first detectable on day 28 (9.3–12.5%) and increased to about 45% (range 43.3–48.9%) by day 149 (Table 4). There were no apparent differences in the radioactivity compositions related to the different doses administered.

Retinal concentrations of intact GEM132 (total radioactivity × purity × fraction in region A) as a function of time are shown in Fig. 1. Analysis of the retinal concentrations of intact GEM132 within each respective dose group (Tukey-Kramer honestly significant difference test, JMP Statistical Discovery Software, Version 3.1; SAS Institute, Inc., Cary, NC) indicated no statistically significant differences between the concentrations at 29 and 56 days postdosing. GEM132 concentrations in the retina increased from 7 days (first sample) to the following apparent maximum values at 56 days postdose: 23.8 ± 3.5 μg Eq/g (low-dose), 84.8 ± 11.3 μg Eq/g (mid-dose), and 448.1 μg Eq/g (high-dose). Subsequently, at the last sampling time, concentrations of GEM132 in the retina were lower: 8.8 ± 3.5 μg Eq/g (low-dose), 26.3 ± 5.4 μg Eq/g (mid-dose), and 131.0 μg Eq/g (high-dose).

The localization and relative concentration of radioactivity in the retina were visualized as small, reduced silver grains lying on the cellular surface. Representative photographs resulting from these microautoradiography studies are shown in Fig. 3. The largest amount of radioactivity was observed in the middle layers of the retina, comprising the inner and outer nuclear layers and the outer plexiform layers. The following gradient of radioactivity distribution was consistently observed in the retina: less radioactivity was observed in the ventro-anterior (ventro-rostral) portion than in the posterior (caudal) and dorso-rostral portions of retinal tissue. Radioactivity was also

TABLE 2

GEM132 AUC and relative AUC ratios for retina, vitreous humor, and remaining ocular tissue after a single intravitreal injection

Dose	Dose Ratio	Retina[a]		Vitreous Humor[a]		Remaining Ocular Tissue[a]	
		AUC_{7-t}	AUC Ratio	AUC_{7-t}	AUC Ratio	AUC_{7-t}	AUC Ratio
μg/eye		*μg Eq · day/g*		*μg Eq · day/g*		*μg Eq · day/g*	
3.7	1	835	1	4.6	1	53.1	1
15.7	4.2	3,210	3.8	10.5	2.3	218	401
78.5	21.2	19,500	23.4	84.2	18.3	1,100	20.7

[a] AUC was calculated by the trapezoidal rule from 7 to 149 days (low- and mid-dose groups) and 7 to 114 days (high-dose group) using the mean concentration obtained from three eyes per time dose. As each time point was the mean of three eyes from individual animals, only a single estimate of the AUC for each dose was obtained.

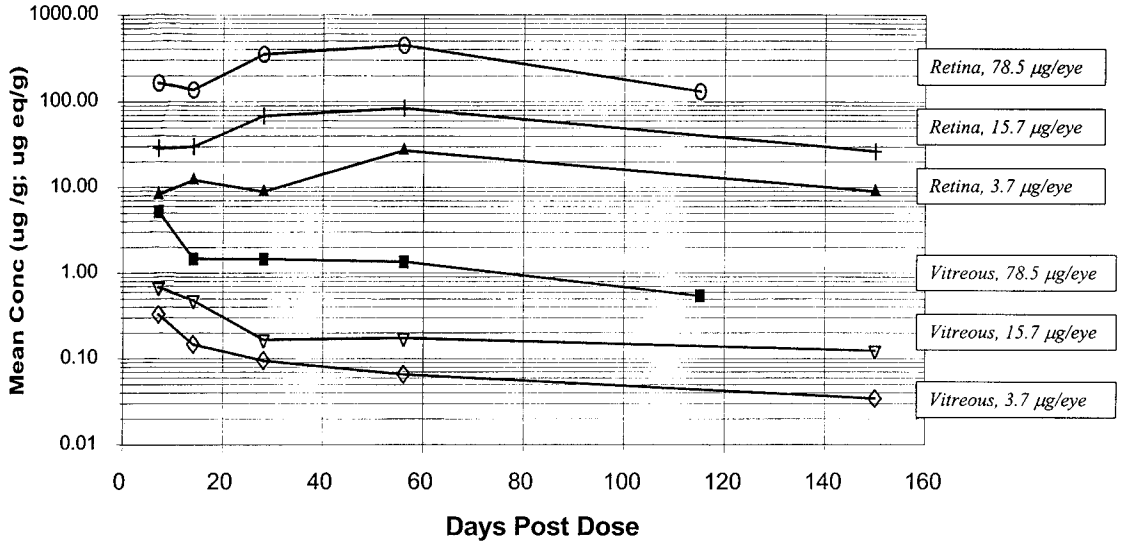

FIG. 1. *Mean concentration of GEM132 in retina and total radioactivity in vitreous after a single intravitreal injection of GEM132 to rabbits.*

TABLE 3

Percentage of dose (S.D.) in vitreous humor, retina, and remaining ocular tissue after a single intravitreal injection of GEM132

Days Postdose	Dose (μg/eye)								
	3.7			15.7			78.5		
	Vitreous Humor	Retina	Remaining Ocular Tissue	Vitreous Humor	Retina	Remaining Ocular Tissue	Vitreous Humor	Retina	Remaining Ocular Tissue
7	6.7 (2.5)	8.5 (5.6)	53.9 (5.2)	3.0 (1.5)	4.6 (1.8)	48.3 (14.3)	5.0 (0.4)	5.8 (1.7)	51.5 (1.9)
14	4.1 (1.1)	12.2 (7.3)	47.5 (1.2)	1.1 (0.5)	5.7 (2.6)	43.3 (22.3)	1.6 (1.1)	8.7 (4.2)	45.8 (11.4)
28	0.62[a]	5.6 (6.0)	41.1 (14.1)	0.61 (0.43)	11.9 (1.8)	48.3 (4.1)	1.1 (1.0)	9.2 (1.7)	41.4 (8.0)
56	0.96 (0.33)	21.8 (3.7)	38.9 (6.2)	0.88 (0.60)	19.4 (10.2)	29.3 (12.0)	1.3 (0.8)	15.9[a]	34.7 (2.1)
114/149[b]	0.97 (0.22)	9.6 (4.9)	37.7 (4.2)	0.75 (0.06)	11.4 (4.2)	36.4 (3.7)	0.28 (0.04)	6.8 (1.6)	41.0 (1.9)

[a] Mean, $n = 2$. For all other values $n = 3$.
[b] For the low- and mid-dose groups, the last time point was 149 days postdose. For the high-dose group, the last time point was 114 days postdose.

TABLE 4

Phosphor image analysis of radioactivity in the retina of rabbits after a single intravitreal injection of GEM132

Days Postdose	Dose (μg/eye)								
	3.7			15.7			78.5		
	A	B	C	A	B	C	A	B	C
	Percentage of total sample radioactivity in gel regions[a] (mean, S.D.)								
7	ND	ND	ND	ND	ND	ND	100 (0)	0	0
14	100[b]	0	0	100 (0)	0	0	94.7 (4.7)	5.3[b]	0
28	87.6[b]	12.5[b]	0	90.7 (2.1)	9.3 (2.1)	0	86.1 (0.7)	13.9 (0.7)	0
56	79.0 (10.6)	20.1 (10.6)	0	69.4 (3.9)	19.8 (9.9)	10.8 (9.8)	71.6 (8.9)	15.5 (3.8)	13.0 (5.2)
114/149[c]	51.1 (1.5)	48.9 (1.5)	0	46.1 (2.6)	42.3 (11.9)	11.6 (10.7)	45.1 (10.4)	35.1 (2.8)	19.8 (7.6)

ND, not determined.
[a] Region A, radioactivity with the same mobility as GEM132 and n-1 + n-2 impurities/metabolites. Region B, radioactivity of impurities/metabolites of chain length $n \geq 3$. Region C, radioactivity of molecular species with higher molecular mass than GEM132. Values reflect the percentage of the radioactivity in the extracted samples migrating in each region.
[b] Mean, $n = 2$.
[c] For the low- and mid-dose groups, the last time point was 149 days postdose. For the high-dose group, the last time point was 114 days postdose.

observed in the optic disk, including the wall of the merangiotic retinal blood vessels, and the amount appeared to be larger at the inner surface of the optic disk. Retinal degeneration, sufficient to obscure the normal inner layering of the retina, was observed in most of the high-dose animals.

Discussion

This report is the first to describe the combined disposition profile and toxicity for a mixed backbone oligonucleotide after intravitreal administration. Although the disposition and toxicity arms of these studies were, in fact, run in different groups of animals and with slightly different dose levels, there were numerous remarkable consistencies in the patterns of responses in the eyes and the patterns of radiolabeled drug distribution.

After intravitreal administration, GEM132 distributed rapidly out of the vitreous into the retina and remaining ocular tissue. Although concentrations in the retina were greater than those in the remaining ocular tissue, the large difference in weight between these two tissue masses (remaining ocular tissues/retina ~50:1) most likely explains why the fraction of the dose present in the remaining ocular tissues is

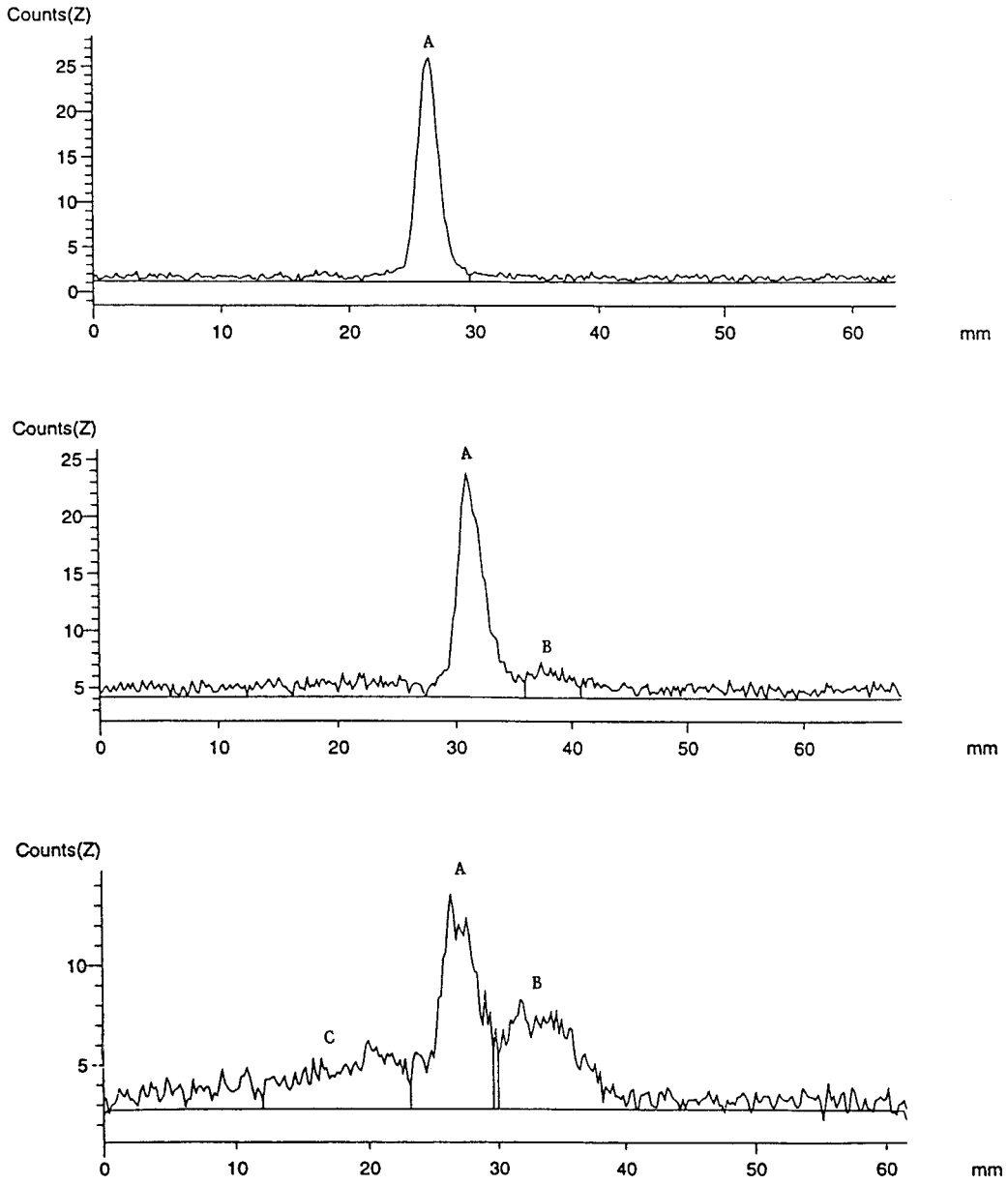

FIG. 2. *Representative PAGE/phosphor image scans of radioactivity in rabbit retina after a single intravitreal injection of 14C GEM132 to rabbits.*

Top, calibration standard; middle, high-dose, day 29; bottom, high-dose, day 114. Region A, radioactivity with the same mobility as GEM132 and n-1 + n-2 impurities/metabolites. Region B, radioactivity of impurities/metabolites of chain length $n \geq 3$. Region C, radioactivity of molecular species with higher molecular mass than GEM132.

greater than that in the retina. The reasons for the apparent increased uptake (on a per gram of tissue basis) of GEM132 by retinal tissues compared with the remaining ocular tissue may reflect unequal distribution of GEM132-associated radioactivity within the remaining ocular tissue. Autoradiography of frozen sagittal sections of rabbit eyes indicates that 5 days postdose, radioactivity in the remaining ocular tissue was associated primarily with the iris/ciliary body (data not shown).

The clearance of GEM132 from the vitreous humor followed apparent first-order kinetics. The estimated half-life for GEM132 in the vitreous humor was about 48 h. This is similar to that reported for other compounds of similar molecular weight (Sirossian et al., 1995; Leeds et al., 1997). Given the enhanced stability of MBOs (Agrawal et al., 1997a; Chen et al., 2000), the data reported here suggest that the clearance of GEM132 from the vitreous humor is primarily due to distribution to ocular tissues and via outflowing aqueous humor. The radioactivity in the vitreous humor at time points beyond 14 days postdose were below the sensitivity of the methodology, and therefore data are not available regarding the profile of the radioactivity in this ocular compartment.

After administration of the lowest dose (3.7 μg), retinal concentrations of GEM132 at 7 days postdose reached a value equal to about 10 times the IC_{90} (1.2 μM, 8 μg/g, Fig. 1). Retinal concentrations of intact GEM132 reached a maximal value 56 days postdose (4.1 μM, 26.9 μg/g) and persisted at levels ~10 times the IC_{90} for months (Fig. 1). The observation that retinal levels of metabolites increased with time, approaching 50% of the total radioactivity in the retina, suggests that clearance of GEM132 metabolites from the retina was slower than their rate of formation.

The single, bilateral administration of GEM132 at a dose level of 5

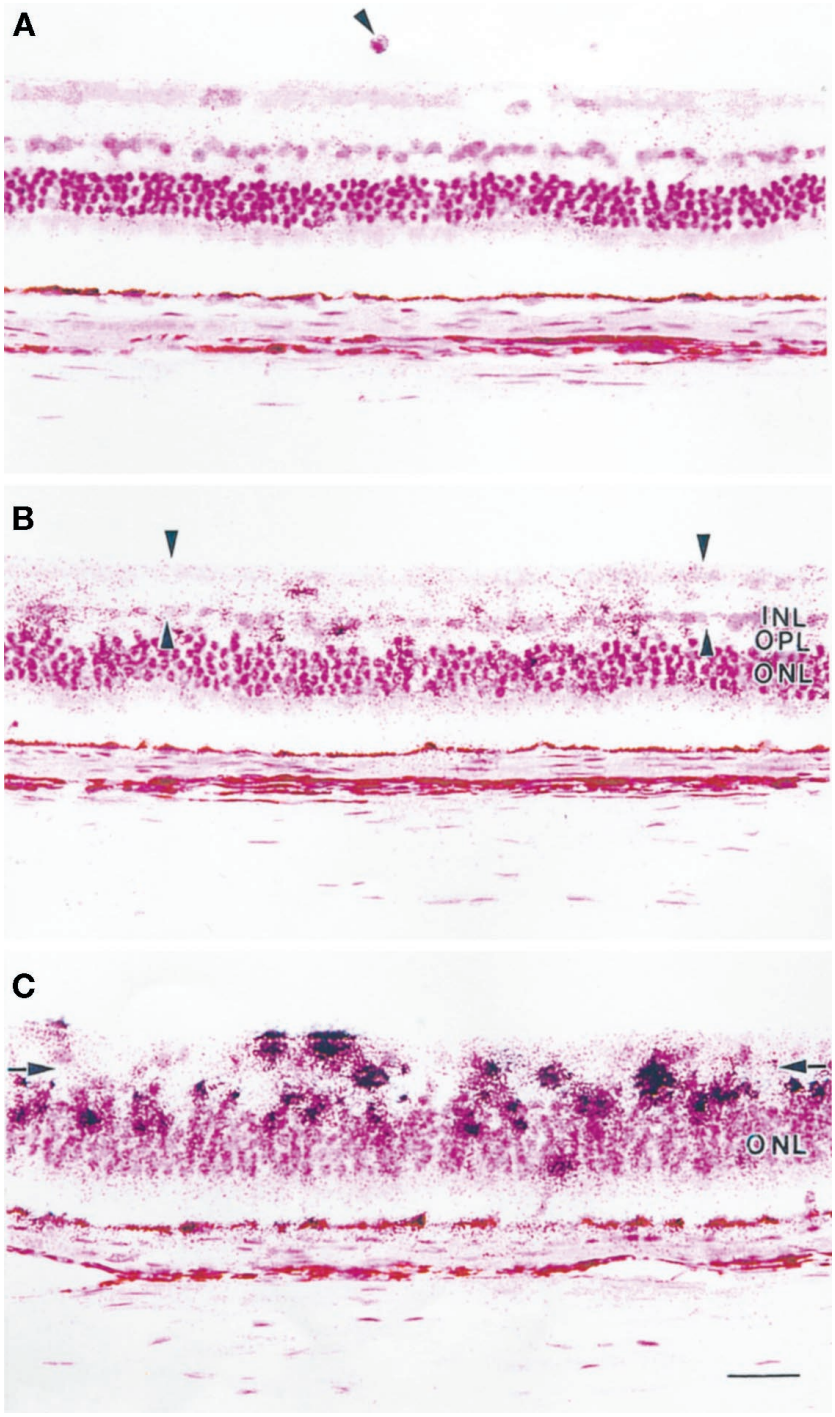

FIG. 3. *Microautoradiography of the ventral retina from rabbits 56 days after a single intravitreal injection of [^{14}C]GEM132.*

H&E. Bar, 30 μm. A, low-dose animal. Slight radioactivity in most retinal layers; one radioactive mononuclear cell in the vitreous humor (arrowhead). B, mid-dose animal. Radioactivity is more intense in outer nuclear layer (ONL), outer plexiform layer (OPL), and inner nuclear layer (INL) than in other retinal layers. Superficial retinal atrophy is noted (between arrowheads). C, high-dose animal. Superficial retinal atrophy is marked with disruption of inner nuclear layer (arrows). Note the strong and patchy distribution of the radioactivity in the outer nuclear layer (ONL) and more inner layers of the retina.

μg/eye did not result in any adverse test article related effects. Although clinical ophthalmological evidence of retinal toxicity was seen in a few animals receiving 20 μg/eye, decreased potential by ERG suggests a higher incidence of functional retinal changes persisting for up to 20 weeks postdose. At a dose of 100 μg/eye, there was clear evidence of retinal toxicity in the form of severely decreased ERG electrical potential and retinal degeneration observed during the ophthalmology exams and microscopic pathology present for up to 16 weeks postdose. Due to the severely decreased ERG potential observed at 16 weeks in the high-dose group (Table 1), we chose to terminate this group at this time. The decreased ERG potential that persisted for up to 20 weeks in the mid-dose group (Table 1) was the reason we chose to terminate the mid- and low-dose groups at week 21.

Figure 3 shows the distribution profile in the retina for [^{14}C]GEM132 in each dose group evaluated 8 weeks after dosing. In

the low-dose group, there was only slight radioactivity in most retinal layers (GEM132 retinal concentration, 24 μg/g). Correspondingly, there was no significant pathology or functional toxicity evident in the eyes of animals from that low-dose group. In the mid-dose group, radioactivity was more intense in both the inner and outer nuclear layers and the outer plexiform layer (GEM132 retinal concentration, 85 μg/g). In the toxicology study, slight to mild retinal degeneration, characterized by a partial disorganization at the outer and inner plexiform layer and the ganglion cell layer, was evident in both the mid- and high-dose animals by 4 weeks postdose (high-dose; GEM132 retinal concentration, 350 μg/g) or 8 weeks postdose (mid-dose). In addition, by 16 weeks postdose, both eyes in high-dose animals showed slight to mild retinal degeneration at the inner nuclear and plexiform layers, ganglion cell layer, and the optic nerve fiber layer. This is also consistent with the radiolabel distribution seen in Fig. 3, where superficial retinal atrophy was evident in the high-dose, along with more intense and patchy distribution of radioactivity in the outer nuclear layer and the more inner layers of the retina.

ERGs were performed at regular intervals during the course of the toxicology study. Effects on B-wave amplitude and increased white flicker latency were indicative of a loss of function of the rods and cones, and, while the effect tended to remain stable throughout the observation period, there was no evidence of recovery to levels comparable with control values. This functional observation is consistent with the microscopic evaluations that revealed a basophilic granular material in the retina of both the mid- and high-dose animals. This material was considered to be potentially an accumulation of the test article. The accumulation was also not reversed, as expected from the ERG effects and the slow apparent clearance of radiolabeled compound from the retina.

A comparison of the ocular disposition of the MBO GEM132 after administration of 3.7 μg/eye and the PS oligonucleotide ISIS 2922 at 66 μg/eye (Leeds et al., 1997) indicate that both are cleared rapidly from the vitreous with similar half-lives. Retinal concentrations of GEM132 and ISIS 2922 at C_{max} were about the same (3.5 and 4.1 μM, respectively), although the time to achieve C_{max} was later for GEM132 than for ISIS 2922. Despite an 18-fold difference in dose, retinal concentrations of intact GEM132 were greater than that of intact ISIS 2922 at the comparable time points (days 7, 14, 20, and 28). The clearance of GEM132 from the retina was significantly slower than that of ISIS 2922, most likely due, in part, to the enhanced stability of the MBO compared with the PS oligonucleotide. Other factors, such as the presence of four contiguous guanosines (4G motif) may also impact the tissue clearance of the compound (Agrawal et al., 1997b). The combination of the higher oligonucleotide concentration in the retina and slower retinal elimination of GEM132 suggest that less frequent dosing with this MBO compared with the PS oligonucleotide might be required to achieve and maintain therapeutic concentrations above those associated with in vitro antiviral activity.

References

Agrawal S, Jiang Z, Zhao Q, Shaw D, Cai Q, Roskey A, Channavajjala L, Saxinger C and Zhang R (1997a) Mixed-backbone oligonucleotides as second generation antisense oligonucleotides: In vitro and in vivo studies. *Proc Natl Acad Sci USA* **94:**2620–2625.

Agrawal S, Tan W, Cal Q, Xie X and Zhang R (1997b) In vivo pharmacokinetics of phosphorothioate oligonucleotides containing contiguous guanosines. *Antisense Nucleic Acid Drug Dev* **7:**245–249.

Bayever E., Iversen PL, Bishop MR, Sharp JG, Tewarey HK, Areneson MA, Pirruccello SJ, Ruddon RW, Kessinger A, Zon G and Armitage JO (1993) Systemic administration of a phosphorothioate oligonucleotide with a sequence complementary to p53 for acute myelogenous leukemia and myelodysplastic syndrome: Initial results of a phase I trial. *Antisense Res Dev* **3:**383–390.

Chen HX, Marshall JL, Ness E, Martin RR, Dvorchik B, Rizvi N, Marquis J, McKinlay M, Dahut W and Hawkins MJ (2000) A safety and pharmacokinetic study of a mixed-backbone oligonucleotide (GEM231) targeting the type I protein kinase A by two-hour infusions in patients with refractory solid tumors. *Clin Cancer Res* **6:**1259–1266.

Field AK, Pad GS and Martin RR (1997) GEM132-an antisense drug for the treatment of CMV. *Int Antiviral News* **5:**219–222.

Glover JM, Leeds JM, Mant TGK, Kisner DL, Zuckerman J, Levin AA and Shanahan WR (1997) Phase I safety and pharmacokinetic profile of an ICAM-1 antisense oligonucleotide (ISIS 2302). *J Pharmacol Exp Ther* **282:**1173–1180.

Leeds JM, Henry SP, Bistner S, Scherrill S, Williams K and Levin AA (1998) Pharmacokinetics of an antisense oligonucleotide injected intravitreally in monkeys. *Drug Metab Dispos* **26:** 670–675.

Leeds JM, Henry SP, Truong L, Zutshi A, Levin AA and Kombrust D (1997) Pharmacokinetics of a potential human cytomegalovirus therapeutic, a phosphorothioate oligonucleotide, after intravitreal injection in the rabbit. *Drug Metab Dispos* **25:**921–926.

Padmapriya AA, Tang J and Agrawal S (1994) Large-scale synthesis, purification, and analysis of oligodeoxynucleotide phosphorothioates. *Antisense Res Dev* **4:**185–199.

Pari GS, Field AK and Smith JA (1995) Potent antiviral activity of an antisense oligonucleotide complementary to the intron-exon boundary of human cytomegalovirus genes UL36 and UL37. *Antimicrob Agents Chemother* **39:**1157–1161.

Perry CH and Balfour JA (1999) Fomivirsen. *Drugs* **57:**375–380.

Séréni D, Tubiana R, Lascoux C, Katlama C, Taulera O, Bourque A, Cohen A, Dvorchik B, Martin RR, Toumerie C, Gouyette A and Schechter PJ (199) Pharmacokinetics and tolerability of intravenous Trecovirsen (GEM91), an antisense phosphorothioate oligonucleotide, in HIV-positive subjects. *J Clin Pharmaco1* **39:**47–54.

Sirossian S, Usansky JI and Tang-Liu DD (1995) Ocular distribution and elimination of ^{3}H-inulin and 3H2O following intravitreal administration to dutch-belted rabbits. *Pharm Res* **12 (Suppl):** S339.

Stevenson JP, Yao KS, Gallagher M, Friedland D, Mitchell EP, Cassella A, Monia B, Kwoh TJ, Yu R, Holmlund J, Dorr FA and O'Dwyer PJ (1999) Phase I clinical/pharmacokinetic and pharmacodynamic trial of the c-raf-1 antisense oligonucleotide ISIS 5132 (CGP 69846A). *J Clin Oncol* **17:**2227–2236.

Zhang R, Lu Z, Zhao H, Zhang X, Diasio RB, Habus I, Jiang Z, Iyer RP, Yu D and Agrawal S (1995) In vivo stability, disposition and metabolism of a "hybrid" oligonucleotide phosphorothioate in rats. *Biochem Pharmacol* **50:**545–556.